Change in Molecular Conformation of Dibenzo-Crown Ether Induced by Weak Molecule−Substrate Interaction

T. Hosokai,*,† M. Horie,‡ T. Aoki,§ S. Nagamatsu,§ S. Kera,†,§ K. K. Okudaira,†,§ and N. Ueno†,§

Graduate School of Science and Technology and Graduate School of Advanced Integrated Science, Chiba University, Chiba 263-8522, Japan, and Supramolecular Science Laboratory, Riken, Saitama, 351-0198, Japan

Received: November 13, 2007; In Final Form: January 8, 2008

The electronic structure and molecular orientation of dibenzo-18-crown-6 deposited on graphite were studied by ultraviolet photoelectron spectroscopy and metastable atom electron spectroscopy. We observed an alternate orientation of the molecule in the first monolayer and second layer. Moreover, the energy separations of the three top π-bands containing the highest occupied molecular orbital in the first layer were found to be clearly different from those in the multilayers, indicating that the conformation of the molecules in the first layer markedly changes even with a weak molecule−substrate interaction.

1. Introduction

There has been considerable interest in the preparation and characterization of ordered arrays of macromolecules because of their potential applications in organic optoelectronic devices. In particular, an understanding of the influences of the interaction between macromolecules and substrate surfaces on electronic structures and molecular orientation is crucial for controlling the properties of a macromolecule on a substrate.[1−3] In the field of organic semiconductor devices, many studies have been performed using π-conjugated molecules that have a rigid and planar framework. However, there are few studies of the molecular ordering and electronic structures of macrocyclic molecules with a flexible framework although a variety of such molecules have been widely employed as components of molecular mechanical devices.[4,5] Molecular mechanical devices work by changing their electronic structure as well as their molecular conformation in terms of the size of a single molecule. Therefore, detailed studies of the electronic structure, molecular orientation, and conformation of macrocyclic molecules on a substrate are crucial for the construction of desirable molecular mechanical devices.[4−7]

Crown ethers, which consist of flexible cyclic oligoethers, have remarkable properties of recognizing and binding specific metal atoms and ammonium cations in complex mixtures and thus have potential for use in molecular machines.[8−11] In particular, dibenzo-crown ethers, which were initially found in a series of crown ethers by Pedersen,[8] have been employed for the above investigations in solution.[8,9,11] Using in situ scanning tunneling microscopy, Ohira et al. found that dibenzo-18-crown-6(2,3,11,12-dibenzo-1,4,7,10,13,16-hexaoxacyclo-octadeca-2,11-diene) (DB18C6) (Figure 1), which has a large electric dipole with a symmetric molecular conformation (C_{2v}), forms a self-organized two-dimensional structure on a Au(111) substrate in $HClO_4$ solution.[12] To our knowledge, however, few groups have tried to deposit the molecules on a substrate in vacuum and to characterize the electronic structures and orientation of the molecules. The formation and characterization of ordered films of dibenzo-crown ethers on a substrate without a solvent are required not only for device applications but also for understanding the fundamental science of soft molecules.

Here, we report the molecular orientation, electronic structure, and change in the molecular conformation of DB18C6, which was vacuum-deposited without decomposition on a graphite substrate and studied by ultraviolet photoelectron spectroscopy (UPS) and metastable atom electron spectroscopy (MAES). Graphite was employed as the substrate to orient molecules on the surface without inducing a chemical interaction between molecules and the substrate surface, since a graphite surface exhibits large atomically flat terraces and is chemically inert. Hence, DB18C6 on a graphite surface is a typical example of a physisorbed system of dibenzo-crown ethers.

MAES uses metastable atoms as probes, which do not penetrate the bulk of solid, to enable the observation of outermost surface electrons selectively. Its very high surface sensitivity gives direct information on the molecular orientation at the outermost molecular layer.[13,14] Using graphite as the substrate, we can also obtain information on the orientation of polar molecules from the coverage- and thickness-dependent vacuum level (VL) shift in UPS spectra and the molecular electric dipole moment (P) of the target molecule owing to a very weak molecule−substrate interaction.[15,16] The UPS and MAES spectra exhibit features sharper than those in UPS of gas-phase DB18C6 because of reduced thermally induced conformation changes in the gas phase.

The present results demonstrate that DB18C6 molecules orient alternately in the first monolayer and second layer. Furthermore, we found that the electronic structure of the monolayer is different from that of the multilayer owing to a change in the molecular conformation of the monolayer, indicating that the conformation can markedly change even with a weak molecular−substrate interaction because of the flexibility of the molecular framework.

2. Experimental Section

A highly oriented pyrolytic graphite (HOPG/ZYA-grade) was used as the substrate. The HOPG substrate was cleaved in air just before being loaded into the preparation chamber (7×10^{-8} Pa) and cleaned by in situ heating at 673 K for 35 h. DB18C6

* Corresponding author. E-mail: thosokai@graduate.chiba-u.jp.
† Graduate School of Science and Technology, Chiba University.
‡ Riken.
§ Graduate School of Advanced Integrated Science, Chiba University.

10.1021/jp710835b CCC: $40.75
Published on Web 03/05/2008

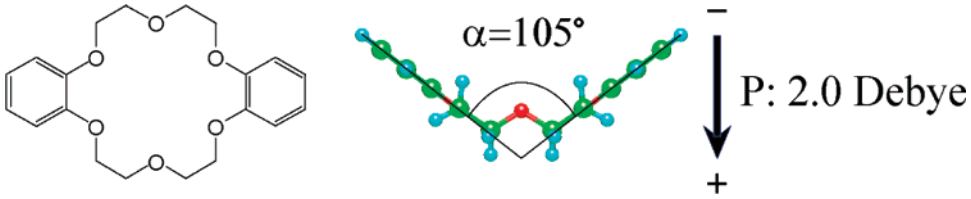

Figure 1. Chemical structure and molecular conformation of DB18C6 (side view) optimized by the DFT (B3LYP/6-311++G**) calculation. The arrow shows the direction of the electric dipole moment (*P*). The calculated value of *P* is 2.0 D.

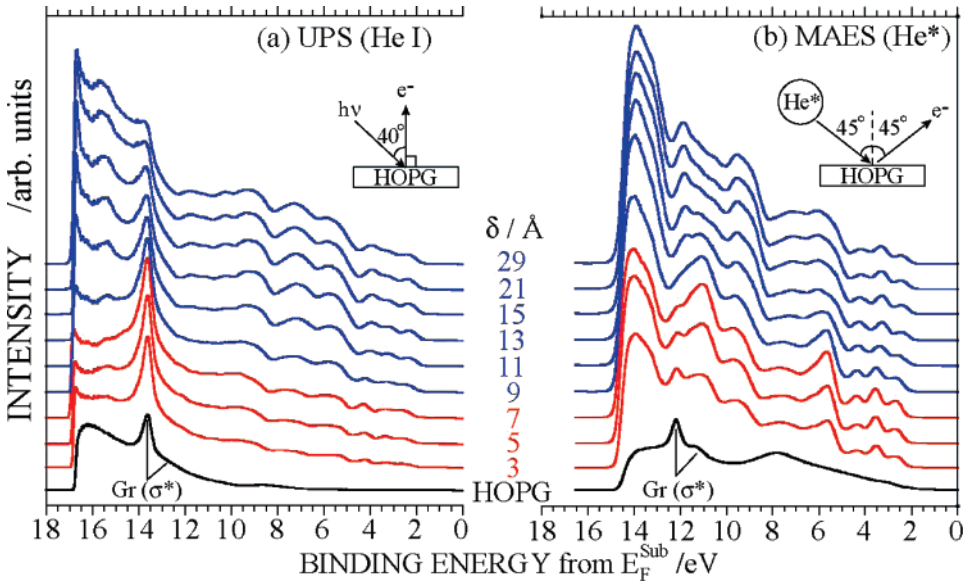

Figure 2. Thickness (δ) dependences of He I UPS (a) and MAES (b) spectra of the DB18C6/HOPG system. The inset in each panel depicts the measurement geometry.

was purchased from Tokyo Chemical Industry Co. (purity > 99.0%) and employed without purification. After sufficient outgassing of DB18C6 in the preparation chamber, thin films of DB18C6 were prepared on the substrate kept at 295 K by sublimation of the outgassed DB18C6 at 358−360 K. The pressure in the preparation chamber was kept below 1×10^{-7} Pa during the sublimation. Deposition amount and rate (0.2−0.3 Å/min) were measured with a quartz microbalance. No decomposition of DB18C6 upon vacuum deposition was observed as confirmed by the high-performance liquid chromatography, ultraviolet−visible absorption spectroscopy and matrix-assisted laser desorption/ionization time-of-flight mass spectroscopy for the vacuum-deposited DB18C6 thin films. This result was also supported by UPS/MAES measurements, which gave clear/sharp spectral features reasonable for undecomposed DB18C6.

MAES and UPS (He I) spectra were measured at 295 K using an ultrahigh-vacuum electron spectrometer[14] with a newly equipped 180° hemispherical analyzer (SPECS-PHOIBOS 100). Metastable He* atoms (2^3S, 19.82 eV; 2^1S, 20.62 eV) were produced by cold discharge of pure helium gas, and the He* (2^1S) component was quenched by a dc helium lamp (quench lamp) to measure the spectra excited by only He* (2^3S). In UPS, the sample was biased at −3.0 V so that the secondary electron cutoff of the spectrum gives the VL. The Fermi level (E_F) was determined from UPS of a thick Au film, and all spectra presented here are displayed using the binding energy (E_B) from E_F of the substrate. The total instrumental energy resolution of the present measurement was set to 120 meV, as measured from the Fermi edge of an evaporated Au film.

3. Results and Discussion

3.1. Molecular Orientation of DB18C6 in a Monolayer and a Bilayer. Figure 2a,b shows the thickness (δ) dependences of the UPS and MAES spectra of DB18C6 on the HOPG substrate, respectively. The UPS and MAES results show different dependences on δ. In the UPS spectra, the intensity of conduction bands of the HOPG substrate (Gr [σ*]) decreases with an increase in δ, whereas in the MAES spectra it disappears completely at $\delta = 9$ Å. The MAES spectra change gradually from 9 to 15 Å and show no change above 15 Å. These results lead to the conclusions that (a) DB18C6 molecules adsorb onto the HOPG substrate to form a monolayer between $\delta = 7$ and 9 Å because MAES spectra reflect the MO distribution at the outermost surface of the films,[13,14] (b) DB18C6 molecules are deposited to form thicker films with further increase in δ, and (c) the molecular orientation of DB18C6 molecules in the monolayer is different from that in thicker films. These conclusions are supported by the VL shift described below.

Figure 3a shows the δ dependence of the VL of the DB18C6/HOPG system obtained from the secondary cutoff positions of the UPS spectra in Figure 2a. As δ increases, the VL shifts to the high E_B side, reaches a maximum at $\delta = 7$ Å by a shift of 0.22 eV, turns back to the low E_B side by 0.16 eV at 15 Å to reach its minimum, and then increases gradually. For a physisorbed molecular layer on an inert surface, the VL is changed by the push-back effect of the substrate,[2,17] and/or the formation of a dipole layer, if each molecule has a dipole (*P*) and the molecules orient similarly on the substrate surface.[15,16] However, because the push-back effect is extremely weak for π-conjugated molecules on a graphite surface owing to a weak van der Waals interaction,[15,16] the observed VL shift for $0 < \delta \leq 15$ Å in Figure 3a is ascribed to the formation of a dipole

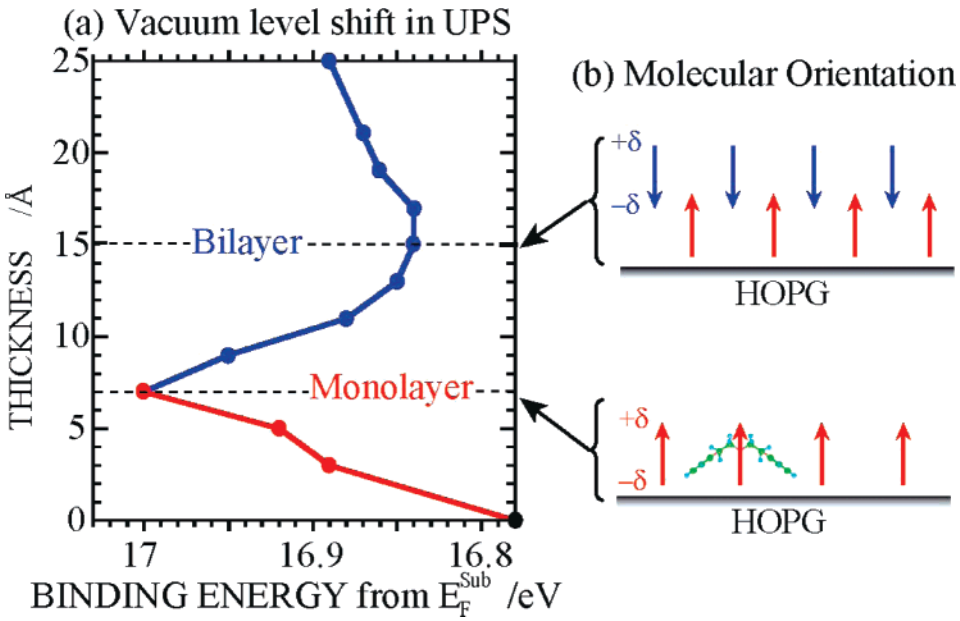

Figure 3. (a) δ Dependence of VL shift measured from the secondary region of UPS spectra. (b) Schematic molecular orientation of DB18C6 on HOPG in monolayer and bilayer estimated by comparing VL shift with dipole direction of DB18C6.

layer by the orientation of DB18C6 molecules in the monolayer (7 Å) and the orientation is opposite of that in the upper layer of the bilayer (15 Å) to cancel the underlying dipoles.[15,16] Because the VL does not recover to its initial value at $\delta = 15$ Å and increases gradually for $\delta > 15$ Å, we expect that the molecular orientation will not be perfect and/or that the packing density/structure will depend slightly on δ for $\delta \geq 15$ Å, which may also induce a change in the dielectric constant (ϵ) of the thin molecular layers. From the consistency between the molecular orientation obtained by MAES and the VL shift, however, an important phenomenon occurring in the DB18C6/HOPG system is the formation of dipole layers for $0 < \delta \leq 15$ Å. Considering the direction of P of DB18C6 as schematically shown in Figure 1, we can thus understand that molecules in the monolayer (7 Å) orient with the cyclic oligoether directed outward to the vacuum region (*upward orientation*), whereas surface molecules in the bilayer (15 Å) orient with the cyclic oligoether directed inward to the substrate (*downward orientation*) (see schematic molecular orientation in Figure 3b).

Figure 4a shows a comparison of the MAES spectra of the 7 Å (monolayer) and 15 Å (bilayer) films, and UPS spectrum of the 7 Å film, in which the electronic density-of-state (DOS) and molecular orbital (MO) energies of a free DB18C6 molecule (C_{2v}) calculated using the density functional theory (DFT) (B3LYP/6-311++G**) are also compared. As understood from the upper valence band features at $E_B = 2-5$ eV in the MAES spectra, the 15 Å MAES spectrum is slightly shifted by about 0.23 eV compared with that of the 7 Å MAES spectrum. This small shift, which is also observed in UPS, may be due to a small difference in the intermolecular interaction in the ionized state between the monolayer and the bilayer. As the molecular orientation of DB18C6 in the monolayer is opposite of that in the upper layer of the bilayer, we expect the intensity of MAES features should reflect the different molecular orientations in the 7 and 15 Å films. In the case of *upward orientation* (monolayer), the intense bands should originate mainly from MOs distributed at the cyclic oligoether part, whereas in the case of *downward orientation* (bilayer) they originate from MOs distributed mainly at two benzene ring parts. We classify the calculated MO states into three types considering the MO distribution as shown in Figure 4a: MOs at two benzene rings (i), those at the cyclic oligoether part (ii), and those spread over both parts (i and ii). In the UPS spectrum, we simply label the observed bands as A−H. Kajitani et al. measured the UPS of gas-phase DB18C6, which is compared in Figure 4a, and reported that bands A and B are ascribed to the π-orbitals of benzene rings, and bands C and D are n(O) localized at an ether ring.[18] Unfortunately, however, they could not assign bands E−H, probably because the separation of bands E−H in the gas-phase spectrum was not sufficient. Note that band C of the thin films is clearly sharper than that of the gas phase, suggesting that the molecular conformation in the gas phase is not unique. Owing to the many closely existing orbitals in the energy regions of bands E−H, the assignments of UPS bands are generally difficult. As understood from Figure 4a, however, the UPS spectrum of the film shows excellent agreement with the calculated DOS over the whole valence region. This can lead to the notion that bands E−H can be assigned as follows by comparison with the calculated results. Band E is ascribed to σ(C−C) and σ(C−H) distributed at (i), (ii), and (i and ii), and π(benzene) at (i); band F to σ(C−C) and σ(C−H) at (i), (ii), and (i and ii), and pseudo-π (O−CH) at (ii); band G to σ(C−C) and σ(C−H) at (i and ii), and pseudo-π (HC−CH) at (ii); and band H to σ(C−H) at (ii) (for definition of pseudo-π, see ref 19).

In the MAES spectra of the 7 and 15 Å films, on the other hand, we observed clearer peaks for the energy regions of UPS bands D and F−H. In the 7 Å MAES spectrum, the intense peaks D′ and G′ are observed in the regions of bands D and G, whereas in the 15 Å spectrum strong peaks F′, F″, and H′ are observed in the regions of bands F and H, respectively. MAES gives clearer peaks even in the band F−H regions than UPS, since He* selectively interacts with MOs existing outermost surface of each DB18C6 layer. Therefore, considering the molecular orientation in the monolayer and second layer shown in Figure 4c, the observed MAES bands can be assigned consistently as follows. For the monolayer (7 Å, *upward orientation*), band D′ originates from n(O) localized at (ii), and band G′ originates from pseudo-π (HC−CH) at (ii). For the bilayer (15 Å, *downward orientation*), bands F′, F″, and H′ are mainly ascribed to σ(C−H) at (i). The MO distributions of these bands are shown in Figure 4b. The observed bands in both UPS

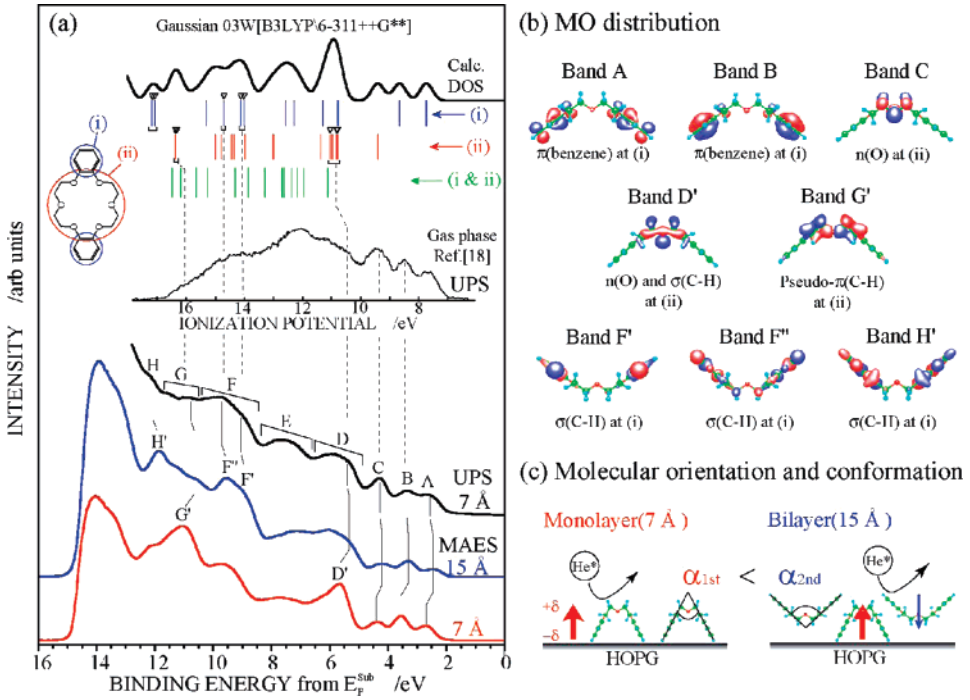

Figure 4. (a) MAES spectra of 7 and 15 Å DB18C6 films, and UPS spectrum of 7 Å DB18C6 film on HOPG. Calculated DOS and MO energies obtained by DFT calculation (B3LYP/6-311++G**) and gas-phase UPS spectrum[18] are also shown for comparison. Bars are molecular levels divided into three groups: MOs distributed at benzene rings (i), at ether ring (ii), and spread over the molecule (i and ii). The bars with open triangles correspond to the MO levels of bands D′ and F′−H′. (b) Spatial distributions of important MOs. (c) Schematic molecular orientation and dipole direction of DB18C6 molecule in 7 and 15 Å films, where expected molecular conformation in the first monolayer is also considered (section 3.2). Each of the three bands [A (HOMO), B (HOMO-1), and C (HOMO-2)] consists of nearly degenerated two π states [one of these two states is shown in (b)].

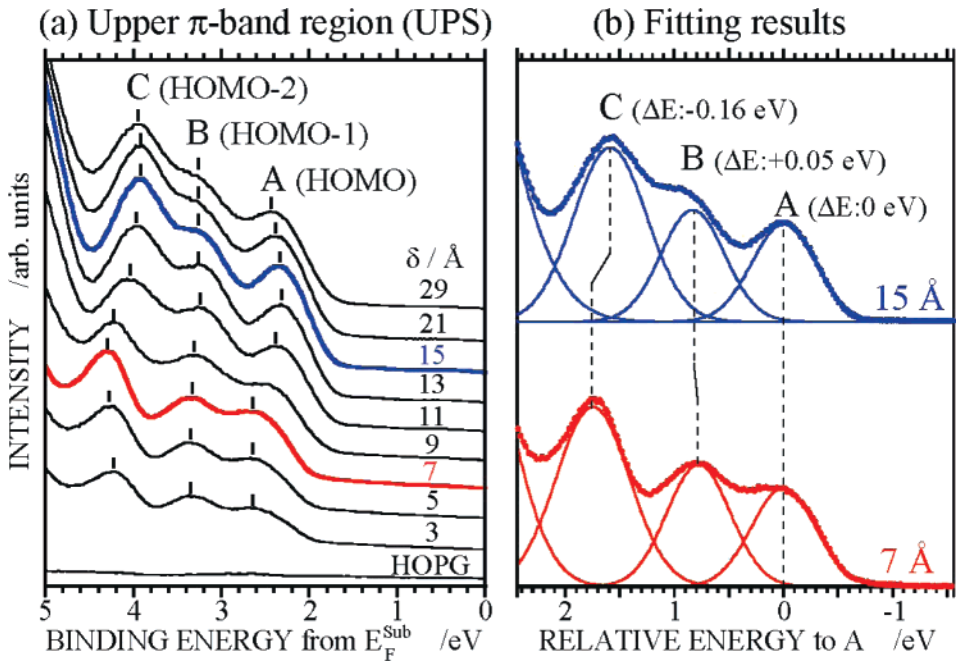

Figure 5. (a) δ Dependence of UPS spectra in the upper valence band region of the DB18C6/HOPG system. (b) Expanded UPS spectra of 7 and 15 Å films with fitting curves as obtained using Gaussian functions, in which the two spectra are compared using relative energy from band A (HOMO).

and MAES spectra are thus reasonably assigned by considering molecular orientations and MO calculation.

3.2. Change in Molecular Conformation of DB18C6 in Monolayer and Bilayer. Figure 5a shows the δ dependence of the UPS spectra of the DB18C6/HOPG system in the upper π-band region, where bands A (HOMO), B (HOMO-1), and C (HOMO-2) are shown. Note that in addition to the shift in the energy positions of these three bands to the low E_B side for 9 Å < δ < 15 Å, the relative energy positions of the bands at 15 Å are clearly different from those at 7 Å. For the 7 Å film, bands A and B are observed at E_B = 2.56 and 3.34 eV, and their peaks are shifted to the low E_B side by 0.23 and 0.18 eV for the 15 Å film, respectively. On the other hand, band C is largely shifted to the low E_B side by 0.39 eV from the 7 Å film to 15 Å film. To understand what happens with the three bands in the 7 and 15 Å films, the expanded spectra of the both films

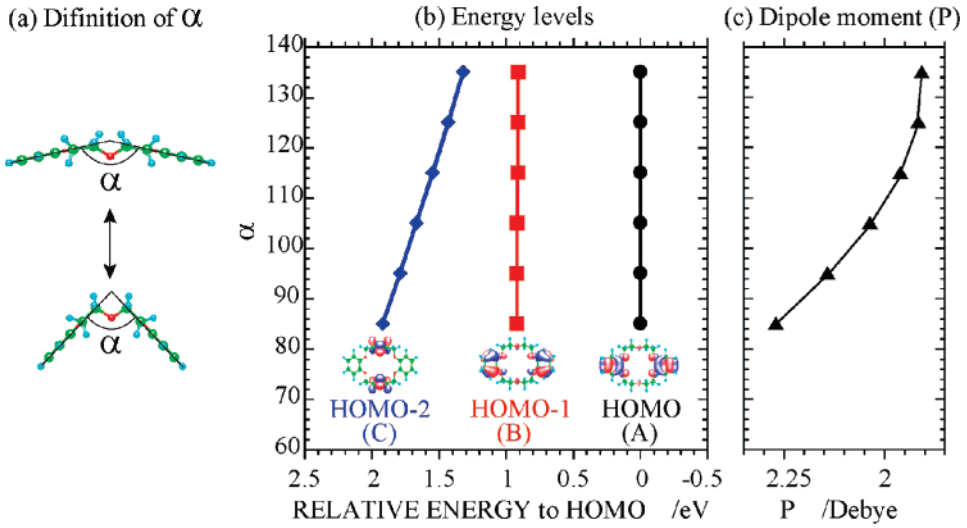

Figure 6. Conformation dependences of molecular energy levels [HOMO (A), HOMO-1 (B), and HOMO-2 (C)] and molecular dipole moment (*P*) calculated with the DFT [B3LYP/6-311++G**]. (a) Examples of DB18C6 conformations with different angles (α) between two benzene rings. (b) α Dependences of energy positions of HOMO-1 and HOMO-2 relative to that of HOMO. (c) α Dependence of *P*. The insets in (b) show spatial MO distributions of HOMO, HOMO-1, and HOMO-2.

are compared in Figure 5b with fitting curves plotted using Gaussian functions. In this comparison, we selected the 15 Å spectrum as a typical spectrum of multilayer films because the spectral shapes and relative positions of the three bands in this spectrum are nearly the same above 15 Å. It is clear from Figure 5b that only band C shifts to the lower E_B side to approach band A; band B stays almost unchanged.

For the marked changes in the relative energy positions of those bands, one must consider a change in the molecular conformation in these two films and both the initial- and final-state effects on the photoionization of molecules on a substrate surface. The initial-state effect generally appears when the electron system is stabilized by intermolecular interaction to result in an increase in E_B and ionization energy. This is not adopted for the above-described relative energy shift, since ionization energy does not increase as understood from the VL and E_B of the UPS features. The final-state effect is related to the screening of photogenerated holes. As established in rare-gas adsorption systems, photoelectrons from a weakly adsorbed multilayer allow the labeling of the first two or three layers through a layer-dependent line shift to the high E_B side owing to a decrease in the screening of the photohole caused by the image-charge final-state effect.[20] However, the observed energy-level shifts in Figure 5a,b are opposite to this final-state effect even if we consider that the average position of the hole distributions of band C is different from those of bands A and B in the molecule (see MO distributions for these three bands in Figure 4b). Another possible final-state effect is the thickness dependence of polarization/relaxation energy.[21,22] This effect might contribute to a change in relative energy position, because photogenerated holes exist at different sites within the molecule for bands C and A + B. However, this effect is considered to be small, since the relative energy difference between these bands shows only very small changes for $\delta > 15$ Å, where the polarization of neighboring molecules must reflect this effect. Accordingly, we must consider the change in molecular conformation as the main origin of the marked shifts in the relative position of band C for the following reasons. Band C is clearly broader in the gas phase than in the film (Figure 4a). This suggests that there are various molecules with slightly different conformations in the gas phase because of the flexibility of DB18C6. As can be seen in Figure 3a, furthermore, the VL in the 15 Å film does not fully return to that of the HOPG, indicating that the dipole-induced potential of the second layer is different from that of the 7 Å film (first layer).

The flexibility of crown ethers was studied by theoretical calculations.[23,24] The results of the studies indicate that the conformation of crown ethers can be changed easily by the binding of alkali atoms and solvent molecules and by increasing temperature. From the theoretical calculation of molecular vibrations using DFT [B3LYP/6-311++G**], we found that a free DB18C6 molecule exhibits a bending vibration that has the lowest vibration energy. This suggests that a sensitive change appears in the angle (α) between the two benzene rings (Figure 6a) by introducing a weak perturbation. We thus simulated the relative energy positions of bands A (HOMO), B (HOMO-1), and C (HOMO-2) and *P* as a function of α by DFT calculation. The results are shown in Figure 6b,c, where the α dependences of the energy positions of bands B and C relative to band A and *P*, respectively, are shown. It is clear that the energy position of C relative to that of A shows a strong α dependence, whereas the energy position of B is almost independent of α. Furthermore, *P* decreases with α. The observed relative energy shift of band C (0.16 eV) reasonably corresponds to a decrease in α from 105° (for optimized ground state conformation) to 98.3° accompanied by a slight increase in *P* by 0.07 D. Although the computed increase in *P* (0.07 D) following the expected decrease in α (105−98.3°) is too small in comparison with the residual surface potential (the VL shift) at $\delta = 15$ Å, the calculated results are qualitatively consistent with both the relative energy shift of band C between the 7 and 15 Å films and the direction of the observed VL shift. Therefore, we conclude that (i) the α of DB18C6 in the 7 Å film (monolayer) is larger than that in the upper layer of the 15 Å film (bilayer) as illustrated in Figure 4c, and (ii) this conformation change is induced by the weak interaction between the molecules and the substrate.

4. Conclusions

We used UPS and MAES to study the molecular orientation and electronic structure of DB18C6 films vacuum-deposited on graphite surfaces. We observed an alternate orientation of molecules in the first monolayer and second layer. Furthermore, we obtained evidence that the electronic structures of DB18C6

in the monolayer differ from those in the second layer. The different electronic structure of the molecules in the monolayer can be explained by the change in the molecular conformation of DB18C6 induced by a weak molecule−substrate interaction. This is ascribed to the flexibility of oligoether ring in the DB18C6 molecule.

Acknowledgment. The present work was partly supported by a Grant-in-Aid for Young Scientists (A) of JSPS, a JSPS fellowship for Young Scientists, and the 21st COE Program of MEXT (Frontiers of Super Functionality Organic Devices, Chiba University).

References and Notes

(1) Forrest, S. R. *Chem. Rev.* **1997**, *97*, 1793.

(2) Ishii, H.; Sugiyama, K.; Ito, E.; Seki, K. *Adv. Mater*. **1999**, *11*, 605.

(3) Salaneck, W. R.; Seki, K.; Kahn, A.; Pireaux, J.-J. *Conjugated Polymer and Molecular Interfaces: Science and Technology for Photonic and Optoelectronic Applications;* Marcel Dekker: New York, 2002.

(4) Balzani, V.; Venturi, M.; Credi, A. *Molecular Devices and Machines: A Journey into the Nano World;* Wiley-VCH: Weinheim, Germany, 2003.

(5) Kay, E. R.; Leigh, D. A.; Zerbetto, F. *Angew. Chem., Int. Ed.* **2007**, *46*, 72.

(6) Deng, W.-Q.; Muller, R. P.; Goddard, W. A. *J. Am. Chem. Soc*. **2004**, *126*, 13562.

(7) Whelan, C. M.; Gatti, F.; Leigh, D. A.; Rapino, S.; Zerbett, F.; Rudolf, P. *J. Phys. Chem. B* **2006**, *110*, 17076.

(8) Pedersen, C. J. *J. Am. Chem. Soc*. **1976**, *89*, 2495.

(9) Stoddart, J. F. *Pure Appl. Chem*. **1988**, *60*, 467.

(10) Zhang, H.; Chu, I.-H.; Leming, S.; Dearden, D. V. *J. Am. Chem. Soc*. **1991**, *113*, 7415.

(11) Ashton, P. R.; Ballardini, R.; Balzani, V.; Gómez-López, M.; Lawrence, S. E.; Martinez-Díaz, M. V.; Montalti, M.; Piersanti, A.; Prodi, L.; Stoddart, J. F.; Williams, D. J. *J. Am. Chem. Soc*. **1997**, *119*, 10641.

(12) Ohira, A.; Sakata, M.; Hirayama, C.; Kunitake, M. *Org. Biomol. Chem*. **2003**, *1*, 251.

(13) Harada, Y.; Masuda, S.; Ozaki, H. *Chem. Rev*. **1997**, *97*, 1793.

(14) Kera, S.; Setoyama, H.; Onoue, M.; Okudaira, K. K.; Harada, Y.; Ueno, N. *Phys. Rev. B* **2001**, *63*, 115204.

(15) Fukagawa, H.; Yamane, H.; Kera, S.; Okudaira, K. K.; Ueno, N. *Phys. Rev. B* **2006**, *73*, 041302(R).

(16) Kera, S.; Fukagawa, H.; Kataoka, T.; Hosoumi, S.; Yamane, H.; Ueno, N. *Phys. Rev. B* **2007**, *75*, 121305(R).

(17) Witte, G.; Lukas, S.; Baqus, P. S.; Wöll, C. *Appl. Phys. Lett*. **2005**, *87*, 263502.

(18) Kajitani, M.; Sugimori, A.; Sato, N.; Seki, K.; Inokuchi, H.; Harada, Y. *Bull. Chem. Soc. Jpn*. **1979**, *52*, 2199.

(19) Kera, S.; Setoyama, H.; Kimura, K.; Iwasaki, A.; Okudaira, K. K.; Harada, Y.; Ueno, N. *Surf. Sci*. **2001**, *1192*, 482.

(20) Kaindl, G.; Chiang, T.-C.; Eastman, D. E.; Himpsel, F. J. *Phys. Rev. Lett*. **1980**, *45*, 1808.

(21) Sato, N.; Seki, K.; Inokuchi, H. *J. Chem. Soc., Faraday Trans. 2* **1981**, *77*, 1621.

(22) Fukagawa, H.; Yamane, H.; Kataoka, T.; Kera, S.; Nakamura, M.; Kudo, K.; Ueno, N. *Phys. Rev. B* **2006**, *73*, 245310.

(23) Glendening, E. D.; Feller, D.; Thompson, M. A. *J. Am. Chem. Soc*. **1994**, *116*, 10657.

(24) Ha, Y. L.; Chakraborty, A. K. *J. Phys. Chem*. **1991**, *95*, 10781.